

# **ROI Based Quality Access Control of Compressed Color Image using DWT via Lifting**

Amit Phadikar\*, Santi P. Maity<sup>+</sup>

*\*Department of Information Technology, MCKV Institute of Engineering, Liluah, Howrah, 711204, India.*

*<sup>+</sup>Department of Information Technology, Bengal Engineering and Science University, Shibpur, Howrah, 711 103, India.*

Received 18th October 2008; accepted 9th July 2009

---

## **Abstract**

Region-of-Interest (ROI) in an image or video signal contains important information and may be used for access control at various qualities using multiresolution analysis (MRA). This paper proposes a novel quality access control method of compressed color image by modulating the coefficients of ROI at various levels. Data modulation causes visual degradation in the original image and plays the key role in access control through reversible process. The modulation information, in the form of a secret key, is embedded in non-ROI part of the chrominance blue ( $C_b$ ) channel of the color image using quantization index modulation (QIM). Lifting based DWT, rather than conventional DWT, is used to decompose the original image in order to achieve two-fold advantages, namely (1) better flexibility and low loss in image quality due to QIM and (2) better decoding reliability that leads to better access control. Only the authorized users having the full knowledge of the secret key restore the full quality of ROI. Simulation results duly support this claims.

*Key Words:* Access Control, Compressed Domain, ROI, Wavelet, Lifting, Watermarking, QIM.

---

## **1 Introduction**

Rapid advancement in digital techniques over the decades had transformed the style of storage and transmission of painting, drawing and other art works from analog form to digital form. Nowadays, digital media such as digital images are generally represented in compressed form like JPEG, more recently in JPEG 2000 format, be it in the digital cameras, World Wide Web alike or audio/video-on-demand on broadcast network channel. The digital data can be duplicated without any quality degradation with respect to their decompressed version. This property of digital technology has also encouraged thieves and discouraged the creator and the owner of the digital art works [1]. Manufacturers and the vendors have always two different objectives in their mind. They need to place their large volume of valuable works in the website for wide publicity and at the same time they want to restrict full quality access to the general users in order to maintain their commercial benefits. This has created a pressing demand to the manufacturers and the vendors to develop a quality access control scheme of the compressed data, which allows all the receivers of the broadcast channel to display a low quality image (or video) with no or little commercial value. But at the same time, the scheme also allows image access at higher quality levels depending on each user's access rights that usually are determined by the subscription agreement.

---

Correspondence to: < amitphadikar@rediffmail.com,santipmaity@it.becs.ac.in>

Recommended for acceptance by < Jean Ogier >

ELCVIA ISSN: 1577-5097

Published by Computer Vision Center / Universitat Autònoma de Barcelona, Barcelona, Spain

Research in access control is now in its very early stage and scrambling, cryptography and visual cryptography are the few widely used methods adopted either to deny or partial accessing of the media. Digital data hiding, although originally developed for copyright protection, ownership verification and authentication are now being used for access control due to commercial or security reasons [1, 2, 3, 4, 5]. In literature, active data hiding (popularly known as watermarking) is commonly used for the former class of applications while the latter purpose is served by passive data hiding methods. Passive data hiding is a technique used for media identification where it is expected that signal distortions caused due to data hiding can be reverted by the authorized users to enjoy the full quality. Access control promises to be an important application in future generation mobile communication system where billing is expected to be performed based on the fulfillment of degree of quality of services (QoS) [2,3].

The need of access control has received widespread attention but a limited number of solutions have been proposed in [6, 7, 8, 9, 10]. Similarly, limited research works focus on the use of data hiding scheme to meet the goal of access control. Access control is normally done through modulation of transform coefficients like discrete cosine transform (DCT), discrete wavelet transform (DWT) etc. of the image and video signals using secret key. *Grosbois et al.* [6] propose an authentication and two access control (on image resolutions and qualities) technique of an image in wavelet domain that can be easily integrated in a JPEG 2000 codec, while remaining compliant with the standard. *Imaizumi et al.* [7] offer a new private-key encryption for JPEG 2000 code streams for flexible access control of layers, resolution levels and color components. *Chang et al.* [8] propose a structure to perform layered access control on scalable media by combining encryption and robust data hiding. *Pickering et al.* [9] suggest a blind data-hiding scheme in complex wavelet for access control of video where compliant DVD player denies access to the pirated copy of video. Recently, *Phadikar et al.* [10] propose a quality access control of gray scale image in DCT compressed domain. The secret key is padded as a metadata at the end of the bit string. However, this may create a risk as the metadata may be lost especially if the content undergoes a variety of format changes.

The majority of the conventional DWT and DCT based access control schemes reported in the literature suffer from few shortcomings. Protection of ROI is not taken into consideration during access control. It is to be noted that ROI of an image, in general, remains intact during many applications like coding and compression in order to preserve its essential value or importance. However, with reverse argument this image feature may be modified if the process is reversible and thus leads to its application in access control. Moreover, access control of compressed image through data hiding is also challenging as the two operations are antagonistic in characteristics. While data hiding uses very redundancy present in the host signal to make embedding imperceptible, compression removes the redundancy and keeps no or less rooms for data insertion. Embedding domain should also be chosen in such a way that the flexibility among the sample coefficients lost due to compression operation may be achieved to a certain extent and can be made use for data hiding. The other shortcoming is high computation complexity that makes the algorithms unsuitable for faster implementation. It is reported in the literature that compared to DCT, conventional DWT has less computational cost [11]. But in the case of an image having large size, it is still a problem when DWT is applied to a whole image [11][12]. The issue becomes important for development of an access control algorithms as the application sometimes demand real time implementation for which hardware realization becomes a viable alternative.

Recently, lifting is used widely for designing fast wavelets and to perform the discrete wavelet transform [13]. The faster computation speed of lifting over conventional DWT makes its hardware implementation easier [13]. Moreover, integer wavelet coefficients cause no loss in signal values during analysis and synthesis. Its mathematical analysis allows a path for creation of correlation among the sample coefficients which may be important for compressed data and may lead to low loss in image information due to data hiding. All these attributes of lifting based DWT may be integrated to develop cost effective access control for compressed image and video signals. Moreover, lifting offers low bit error rate (BER) ( $P_e$ ) in watermark decoding compared to DWT, as the former shows low variance of the cover coefficients compared to the latter [14]. The embedding of secret key permits format conversion to occur without the risk of losing this information and QIM may be chosen for its potentiality of ease of implementation [15].

The present work develops a quality access control scheme by modulating ROI of an image in compressed domain using lifting based discrete wavelet transform (DWT). The modulation information, in the form of a secret key or watermark, is embedded in the non-ROI area of the chrominance blue channel

( $C_b$ ) in the color image using QIM. The secret key, embedded in the form of watermark, is extracted at the user end and is used at the time of decoding for the encoded data. The simulation results show that the users having full knowledge of the key can get the best copy (100% quality with respect to compressed image) of the images, while all other users can only access the images up to a certain level of quality. Simulation results also show that the usage of lifting in access control offers better performance compared to DWT in terms of image visual quality due to the embedding of more number of watermark bit information. Performance of the proposed access control scheme is also compared with the other existing works. Simulation results also show that protection of ROI for the proposed method is much better compared to other existing access control scheme.

The paper is organized as follows: Section 2 describes proposed access control scheme while in Section 3 the performance evaluation of the scheme is demonstrated. Conclusions are drawn in Section 4 along with the scope of future work.

## 2 Proposed Access Control Scheme

The proposed access control scheme consists of two main modules, namely, data encoding and data decoding. The encoding module basically performs *compression*, *modulation* and *symbol encoding* while the decoding module does the reverse operations i.e., *symbol decoding*, *demodulation* and *decompression*. The detailed block diagram representation of the image encoding is shown in Fig.1.

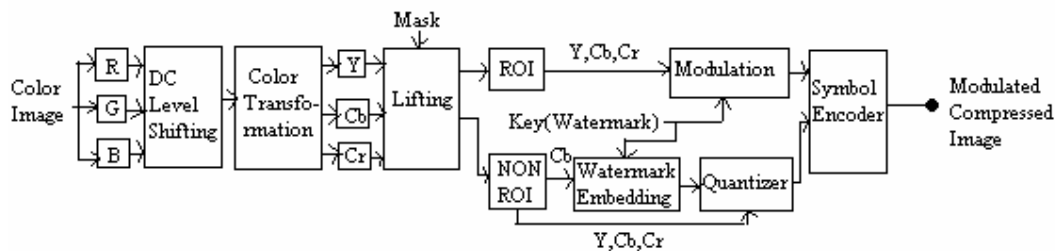


Figure 1: Block diagram of quality access control encoding process

### 2.1 Image Encoding Process

The encoding process consists of the following steps.

#### Step 1: Image Pre-processing

The pixel values of the color components are level shifted by subtracting  $2^{m-1}$ , where 'm' is the number of bits required to represent the gray level of the image. The operation enables the input sample data to obtain a nominal dynamic range centered about zero. This pre-processing operation not only prevents numerical overflow but also makes arithmetic coding, context specification etc. simpler. In particular, this allows the compression more efficient with absolutely no or low loss in image quality. The other advantage offered by this preprocessing step is to develop "hidden QIM" to achieve better possible rate-distortion-robustness performance through a structure that consists of 1) preprocessing of the host signal, 2) QIM embedding, and 3) post processing of the quantized compressed host signal to form the composite signal [15].

#### Step 2: Color Space Transformation

There are several ways to represent color images numerically, for example: *RGB*, *YCbCr*, *CMY*. The symbols *R*, *G*, *B*, *Y*, *C<sub>b</sub>* and *C<sub>r</sub>* denote the red, the green, the blue, the luminance, the chrominance-blue and the chrominance-red, respectively while *C*, *M* and *Y* indicate cyan, magenta, and yellow, respectively. The *CMY* format is preferably used in printing industry and color images are most commonly represented in *RGB* format. In *RGB* format, the image is composed of three component planes; red, green, and blue color components. When the discrete wavelet transformation is applied, each color component is transformed independently. Researchers have reported that for some typical applications, such as image compression, the *RGB* color space is not optimal [16]. It turns out the human brain is more attuned to small changes in terms

of luminance and chrominance (i.e. chrominance blue and chrominance red). A luminance channel carries information regarding the brightness of a pixel. Chrominance is the difference between a color and a reference channel at the same brightness. The most common of these spaces and the one used by JPEG2000 is the  $YC_bC_r$  space. The  $Y$  channel is luminance while  $C_b$  and  $C_r$  are chrominance channels. Moreover,  $Y$ ,  $C_r$  and  $C_b$  color components are less statistically dependent than  $R$ ,  $G$  and  $B$  color components, and hence, they can be processed independently leading to better compression. Therefore, a color transform is performed to convert  $RGB$  data into  $YC_bC_r$  according to the following rule:

$$\begin{pmatrix} Y \\ C_b \\ C_r \end{pmatrix} = \begin{pmatrix} 0.299 & 0.587 & 0.114 \\ -0.16875 & -0.33126 & 0.5 \\ 0.5 & -0.41869 & -0.08131 \end{pmatrix} \times \begin{pmatrix} R \\ G \\ B \end{pmatrix} \quad (1)$$

In brief, this conversion is done as  $YC_bC_r$  color space allows greater compression for the same image quality or better image quality for the same degree of compression operation [16].

### Step 3: Selection of Proper Transform Coefficient

The present scheme uses lifting based DWT rather than conventional DWT for watermark embedding due to the reasons as mentioned in the previous section. We now mathematically analyze how lifting offers benefits in data hiding. Lifting-based filtering consists of a sequence of very simple filtering operations for which alternately odd sample values of the signal are updated with a weighted sum of even sample values and even sample values are updated with a weighted sum of odd sample values [17-19] as shown in Equation 2 and Equation 3 below [20, 21]:

$$y(2n+1) = x_{ext}(2n+1) - \left\lfloor \frac{x_{ext}(2n) + x_{ext}(2n+2)}{2} \right\rfloor \quad (2)$$

$$y(2n) = x_{ext}(2n) + \left\lfloor \frac{y(2n-1) + y(2n+1) + 2}{4} \right\rfloor \quad (3)$$

where  $x_{ext}$  is the extended input,  $y$  is the output signal and  $\lfloor a \rfloor$ , indicate the largest integer not extending 'a' [20,21]. This mathematical form of lifting allows creation of correlation among the sample values. This form of correlation may be beneficial for data hiding on compressed sample coefficients and leads to better image visual quality of the watermarked data. Moreover, lifting offers advantages of low loss in image information in QIM data embedding [14]. It has also been shown that the bit error rate ( $P_e$ ) in watermark decoding, for more general case of M-PAM (M-ary pulse amplitude modulation) signaling, is related to the standard deviation of cover image coefficients [22] as follows:

$$P_e = \frac{2(M-1)}{M} \Upsilon \left( \sqrt{\frac{Nd_0^2}{4\sigma_x^2}} \right) \quad (4)$$

where  $d_0^2$  indicates the watermark power, the value of  $M$  corresponds to M-PAM (for the present case  $M=2$ ),  $\sigma_x^2$  is the variance of pixel values or transform coefficients of image block,  $\Upsilon(\cdot)$  indicates the complimentary error function and  $N$  is the number of cover signal points over which a single watermark bit is embedded. It is seen from the simulation results (Table 7) carried over large number of images that the variance of lifting based DWT coefficients is much lower than the similar for DWT coefficients. This in turn offers low  $P_e$  for the extracted watermark when embedded in the former and this plays an important role in access control through reverse operation. It is also to be mentioned here that lossless compression is an important functionality for a compression scheme like JPEG 2000. Lossless compression is not possible when conventional wavelet transforms are used. This is due to the fact that they map integer-valued image data to real-valued wavelet coefficients. This is another important point that supports the use of lifting over normal wavelets in the present case as the former operation converts integer into integer coefficients.

#### Step 4: Image Transformation

Lifting-based  $n$ -level 2D-DWT is performed on the original image to decompose it into its high and low subbands as shown in Fig. 2 (a). The lifting is performed by filtering each row and column of the pre-processed image with high-pass and low-pass filter. As this process results in double the number of samples, the output from each filter is down sampled by two, so that the sample rate remains constant [16]. The number of levels of wavelet decomposition is implementation dependent; however, three levels are demonstrated in the experimentation. Fig. 2 (b) shows 3-level DWT of the 8-bits/ pixel Lena image tile while Fig. 2(c) shows the same due to lifting based DWT decomposition. Simulation results obtained from experimentation over large number of images show that this number of decomposition levels is good enough to maintain acceptable rate distortion and access control performance through data hiding. We have performed our experimentation using the lifting based 'haar' wavelet for image transformation due to its simplicity and ease of implementation, although other lifting based wavelets can also be used and better results are expected to be achieved. It is also to be argued here that due to the attribute of lossless integer coefficient processing, lifting based operation offers relatively better multiresolution information processing capability compared to the normal DWT operation. This can also be visualized through close look on Fig. 2(b) and Fig. 2(c), respectively.

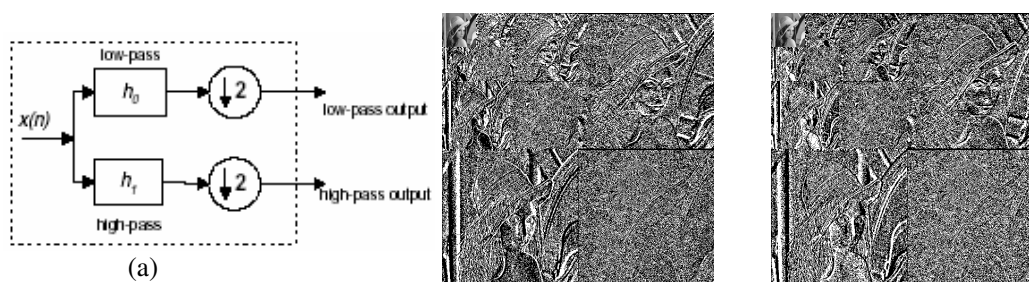


Figure 2: (a) The Lifting based DWT structure; (b) 3-level DWT (haar) of the 8-bit Lena image tile; (c) 3-level lifting based DWT (haar) of the 8-bit Lena image tile.

#### Step 5: Down Sampling

It has been observed that the chrominance components ( $C_r$ ,  $C_b$ ) are less sensitive to human visual system (HVS), which in turn suggests that those components may be down sampled to save space of about 33% or 50% for efficient and compact representation of image [23]. In wavelet domain, the multiresolution nature of wavelet transform may be used to achieve the similar kind of compression effect. For example, if the high-low (HL), low-high (LH), and high-high (HH) subbands of lifting based wavelet decomposition are discarded and all other subbands are retained, a 2:1 sub-sampling is achieved in the horizontal and the vertical dimensions of the component. However, redundancy reduction due to this operation can be compensated to a certain extent in order to achieve flexibility in data hiding through the special mathematical operations laid in Equation 2 and Equation 3. This flexibility helps to maintain better visual quality of the image signals even after data hiding. Moreover, if the luminance component is not used for data modulation, there is no noticeable loss in image quality [20].

#### Step 6: ROI Coding

In region-of-interest (ROI) coding, a selected ROI is mostly restricted to access by the common users than the background [23]. The ROI may be either static or dynamic. Static ROIs are defined at coding time, while dynamic ROIs are defined interactively by the user during a progressive transmission. Generally, a mask is used to define ROIs. The ROI mask essentially indicates which particular set of wavelet coefficients are responsible for access control. Since ROI contains visually significant part of an image, lossless integer coefficients, due to lifting, at different levels allow greater flexibility for the access control to the authorized/unauthorized users. ROI binary mask is supplied by the owner/user. One such ROI binary mask and its 3-level lifting based wavelet domain decomposition are shown in Fig. 3(a) and Fig. 3 (b), respectively. The decomposition of ROI mask in different levels is done in order to make it compatible with

respect to the corresponding decomposition levels of the image signal. The present work uses static mask for ease of implementation.

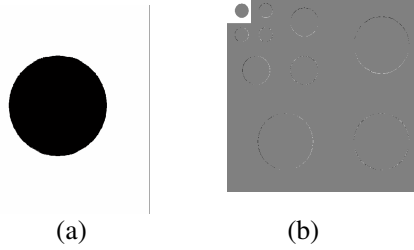


Figure 3: (a) ROI Binary mask examples; (b) 3-scale lifting transformation of (a).

**Step 7: Owner/User Defined Key and its Significance**

The owner/user uses a key (*K*) of length ‘*L*’ bits to develop data modulation on ROI. The most significant ‘*L1*’ number of bits represent the type of channels and the next ‘*L2*’ number of bits represent the number of levels for wavelet subbands to be modulated. The rest of the bits in the key are used to denote the type of modulation to be performed on the coefficients in ROI. Fig. 4 shows a typical sample key of 16 bits length where the first three most significant bits (MSB) (i.e. bit 15-th to 13-th) represent the type of channels and bits 12-th -11-th represent the corresponding lifting based DWT levels to be modulated. We have used 2 bits to represent the level as we decompose the image into three levels. Table-1 and Table-2 represent the respective type of color bands and lifting based DWT levels that are used for modulation.

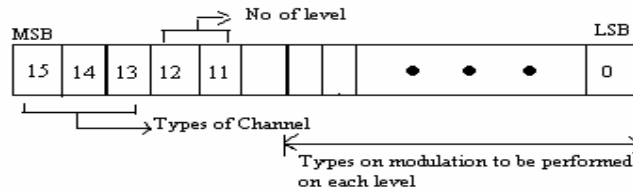


Figure 4: Typical 16 bits user defined binary key (*K*).

Table 1: List of different color bands used for modulation.

Bit 15	Bit 14	Bit 13	Modulation
0	0	0	No
0	0	1	Y
0	1	0	$C_b$
0	1	1	$C_r$
1	0	0	$C_b$ & $C_r$
1	0	1	Y, $C_b$ & $C_r$

Table 2: List of different levels of subbands used for modulation.

Bits 12 & 11	Type of modulation of coefficients in ROI
00	No modulation
01	Only detail coeff. of level-1
10	Detail coeff. of Level -1 and 2
11	Detail coeff. of Level 1,2 and 3

**Step 8: ROI Coefficients Modulation**

The key (*K*) supplied by the owner determines the respective number of levels and the color components of the original data to be modulated. The coefficients which lie in the area of ROI are modulated according to key ‘*K*’. The modulation is done by changing the sign bit of n-level lifting based wavelet coefficients of ROI and is described by the following rule.

$$C^e = (-1) \times C \tag{5}$$

where, *C* and *C<sup>e</sup>* are the quantized lifting based DWT coefficients before and after modulation, respectively. The data modulation offers the following advantages, namely (1) changes in the sign of DWT coefficients may reduce the understandability of images to the unauthorized users and plays the key role in access control of ROI through reversible process, (2) data modification done only in the sign bit of ROI coefficient keeps compression ratio unchanged and leads to the preservation of file size. Moreover, the use of lifting allows

data modulation for integer coefficients, which not only makes quality access control lossless and fully reversible but also offers low cost implementation which may be mapped to real time system through hardware realization [13]. It is found that lifting based operation requires half the computation time required for normal DWT domain operation.

#### Step 9: Efficient and Secured Transmission of the Secret Key

The key ( $K$ ) used in step 7 is embedded as a watermark in the color components as the latter contains large amount of redundant data. Each bit of watermark is embedded in a group ( $G$ ) of high-low (HL) or low-high (LH) coefficients in the chrominance blue ( $C_b$ ) channel as  $C_b$  is less sensitive to human visual system (HVS). The basic idea is that the human eyes are sensitive to the low-low (LL) coefficients and the quantization step of lossy compression may discard the high-high (HH) components. Therefore, the reasonable trade-off between imperceptibility and compression resiliency of the embedded data is achieved by embedding the watermark into the HL or LH coefficients of the image. This is analogous to the usage of middle frequency coefficients for embedding of watermark information in case of unitary transforms like Discrete Fourier Transform(DFT), DCT etc. in order to make a good trade-off between above two requirements of watermarking [24].

#### a): Selection of Step Size and Generation of Binary Dither

Two dither sequences, with length  $L$ , are generated pseudo randomly using a key with the step sizes ( $\Delta_b$ ) as follows:

$$d_q(0) = \left\{ \mathfrak{R}(\text{key}) * \Delta_b \right\} - \Delta_b / 2 \quad \text{where } 0 \leq q \leq L-1 \quad (6)$$

$$d_q(1) = \begin{cases} d_q(0) + \Delta_b / 2 & \text{if } d_q(0) < 0 \\ d_q(0) - \Delta_b / 2 & \text{if } d_q(0) \geq 0 \end{cases} \quad (7)$$

where  $\mathfrak{R}(\text{key})$  is a random number generator. In the present scheme, the value of  $\Delta_b$  is calculated using Equation 10 as shown below. The length of 'L' depends on the number of coefficients in  $G$  that are selected from LH or HL subbands for embedding of each watermark bit.

#### b) Watermark Bit Insertion

The watermark bit is embedded in the middle-frequency coefficients of 2<sup>nd</sup> level, instead of using 1<sup>st</sup> level, as embedding of watermark bit in the latter level may be lost due to down sampling. The  $q$ -th watermarked DWT coefficient  $S_q$  is obtained as follows:

$$S_q = \begin{cases} \mathcal{Q} \left\{ X_q - d_q(0), \Delta_b \right\} + d_q(0) & \text{if } W(i, j) = 0 \\ \mathcal{Q} \left\{ X_q + d_q(1), \Delta_b \right\} - d_q(1) & \text{if } W(i, j) = 1 \end{cases} \quad (8)$$

where  $X_q$  is the  $q$ -th DWT coefficient of the original data,  $\mathcal{Q}$  is a uniform quantizer (and dequantizer) with step  $\Delta_b$ . For QIM based data embedding, the result of the normal wavelet transform can be rounded to integer values and small values may be set to zero. By modifying the result of wavelet transform, perfect invertibility is lost and the original input data cannot be exactly regenerated. However, lifting based operation is perfectly invertible and yields exactly the original data set.

#### Steps 10: Quantization of Wavelet Coefficients

The transform coefficients that lie outside the ROI are quantized using the rule [23] as follows:

$$q_b(u, v) = \text{sign}(a_b(u, v)) \left\lfloor \frac{|a_b(u, v)|}{\Delta_b} \right\rfloor \quad (9)$$

where  $a_b(u, v)$  and  $q_b(u, v)$  denote the coefficients before and after quantization, respectively. The quantization step size  $\Delta_b$  is governed by the following mathematical relation.

$$\Delta_b = 2^{R_b - \varepsilon_b} \left( 1 + \frac{\mu_b}{2^{II}} \right) \quad (10)$$

The symbol  $R_b$  is the nominal dynamic range of subband  $b$ , while  $\varepsilon_b$  and  $\mu_b$  denote the number of bits allotted to the exponent and the mantissa of the subband's coefficients, respectively.

### Step 11: Symbol Encoding

For efficient storage and transmission, all resulting coefficients (both within ROI and non-ROI) are arithmetic and Huffman coded. The code is written in a file and they constitute the compressed and modulated image data.

## 2.2 Image Decoding Process

The decoding process is just reverse to that of the encoding process where input is the modulated compressed Huffman bit sequence. Fig. 5 shows the block diagram representations of image decoding. The steps for decoding process are described as follows.

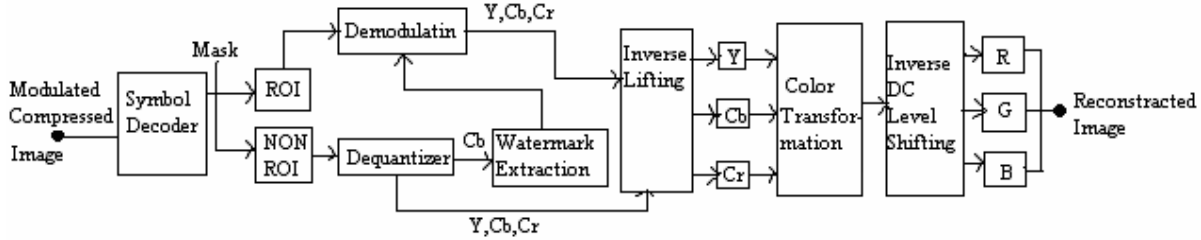


Figure 5: Block diagram of quality access control decoding process.

### Step 1: Symbol Decoding and Separation of Coefficients into ROI and Non-ROI

The entropy decoding is done on the bits sequence to get the modulated quantized DWT coefficients. The DWT coefficients are separated into two groups i.e. ROI and non-ROI coefficients using the knowledge of the mask. Then dequantization is performed on the non-ROI quantized coefficients to get integer DWT coefficients. The separation of ROI and non-ROI coefficients are done to perform different subsequent processing steps for individual.

### Step 2: Key (K) Extraction

The key ( $K$ ) extraction is nothing but the process of watermark decoding. Watermark bits are extracted from the non-ROI area of  $C_b$  channel that are used during embedding. A watermark bit  $\hat{K}(i, j)$  is decoded by examining the group of integer DWT coefficients ( $G$ ) using the following rule.

$$A = \sum_{q=0}^{L-1} \left( \left\lfloor \frac{Q(Y_q - d_q(0, \Delta) + d_q(0) - Y_q)}{2} \right\rfloor \right) \quad (11)$$

$$B = \sum_{q=0}^{L-1} \left( \left\lfloor \frac{Q(Y_q + d_q(1, \Delta) - d_q(1) - Y_q)}{2} \right\rfloor \right) \quad (12)$$

where  $Y_q$  is the  $q$ -th DWT coefficient (possibly distorted due to transmission channel or malicious operations due to unauthorized users) of the received signal. The watermark bits  $\hat{K}(i, j)$  corresponding to a group of selected coefficients ( $G$ ) is now decoded using the following rule.

$$\hat{K}(i, j) = \begin{cases} 0 & \text{if } A < B \\ 1 & \text{otherwise} \end{cases} \quad (13)$$

The extracted bit sequence of watermark ( $\hat{K}$ ) is the secret key used for modulation i.e. the key contains necessary information that had been used for modulating the ROI coefficients to perform access control operation. This key is now used for demodulation in order to reconstruct the image.

### Step3: Demodulation of ROI Components

The key ( $\hat{K}$ ) extracted in step-2 provides the necessary information about the number of subbands and the type of channels to be demodulated to avail full quality of the image. The coefficients, which are within the ROI, are demodulated using ' $\hat{K}$ '. The demodulation is performed according to the following rule.

$$C^{el} = (-1) \times C^e \quad (14)$$

where  $C^e$  and  $C^{el}$  are the quantized integer DWT coefficients before and after demodulation, respectively. This is the reverse operation of step 8 used for encoding process. The restoration of sign for DWT coefficients allows to avail proper visual quality for ROI that plays the key role in access control. Moreover, the quality of restored ROI fully depends on the decoding reliability of the key ( $\hat{K}$ ). Only an authorized user, who has the full knowledge of the key, can restore the full or significant visual quality of the ROI.

### Step 4: Image Transformation

Lifting-based inverse  $n$ -level 2D-DWT is performed on the demodulated ROI coefficients. Inverse transformation maps the transform domain coefficients of  $Y$ ,  $C_b$  and  $C_r$  components in spatial or pixel domain.

### Step 5: Image Post-Processing

The pixel values of the color components ( $Y$ ,  $C_b$  and  $C_r$ ) are inverse level shifted by adding  $2^{m-1}$ , where ' $m$ ' is the number of bits required to represent the gray level of the image. This post-processing operation essentially converts pixel values of the color components over the full dynamic range in order to enjoy the full contrast in visual quality.

### Step 6: Inverse Color Space Transformation

Then  $YC_bC_r$  color components are transformed to get RGB image using the following rule.

$$\begin{pmatrix} R \\ G \\ B \end{pmatrix} = \begin{pmatrix} 1.0 & 0 & 1.402 \\ 1.0 & -0.34413 & -0.71414 \\ 1.0 & 1.772 & 0 \end{pmatrix} \cdot \begin{pmatrix} Y \\ C_b \\ C_r \end{pmatrix} \quad (15)$$

The reverse RGB transformation is done as RGB is an additive color model that is used for light-emitting devices, e.g., CRT (cathode ray tube) displays which are common and widely used display system.

## 3 Performance Evaluation

The performance of the proposed access control scheme is tested over large number of benchmark images [25][26]. All the test images are of size (256x256), 24-bit/pixel-color RGB image and some of them are shown in Fig. 6. The present study uses Peak-Signal-to-Noise Ratio (PSNR)[27] and Mean Structural Similarity Index Measure (MSSIM)(calculated by the average value of SSI of the three-color channels)[28] to quantify the distortion measure as well as quality of the images. We have used 2:1 sub-sampling in the

horizontal and in the vertical dimensions of the components  $C_b$  and  $C_r$  as it is the most commonly used method in all compression schemes.

Fig. 7(a) shows the decoded ‘Pepper’ image obtained after decompression operation without applying the proposed access control. Fig.7 (b) shows the decoded ‘Pepper’ image after watermarking and compression but without modulating the coefficients of ROI. Table 3 lists the bit rate (B.R.), compression ratio (C.R.), PSNR and MSSIM values for some images. The bit rate decreases, as expected, due to quantization based operation done for watermarking.

Table 3: Results for different images without quality access control mechanism.

Image	Only Compression				Compression With Watermarking			
	B.R.	C.R.	PSNR	MSSIM	B.R.	C.R.	PSNR	MSSIM
Pepper	1.51	6.99:1	30.93	0.93	1.48	7.51:1	30.84	0.92
Lena	1.39	8.58:1	33.44	0.93	1.36	9.36:1	33.34	0.92
House	1.53	7.61:1	30.79	0.93	1.50	8.40:1	30.56	0.92
Water	1.54	8.27:1	30.61	0.89	1.52	9.05:1	30.53	0.88

Fig. 7-11 show the results for ‘Pepper’ image when combination of various channels and different levels of subbands are modulated. The subsequent decoded images with and without the usage of true key are also shown. It is seen from Fig. 7-11 that in all test cases, decoded ‘Pepper’ images with the true key are of ultimate quality and the decoded images without the proper key produce a lower level of quality. In other words, the images of Fig. 7(c) and Fig. 8-11(a, c) will be available to all users but the images of Fig. 7(d) and Fig. 8-11(b, d) will only be available to the authorized users who have the subscription agreement. The PSNR values for the images are 23.11dB (Fig.7(c)), 30.56dB (Fig. 8(a)), 29.78dB (Fig. 8(c)), 29.63 dB (Fig.9 (a)), 28.07 dB (Fig.9(c)), 29.42dB (Fig.10 (a)), 27.47dB (Fig.10(c)), 25.33dB (Fig.11 (a)), 22.65dB (Fig. 11(c)). The similar qualitative measures are for 30.84 dB (Fig. 7(d)), 30.84 dB (Fig.8 (b)), 30.84 dB (Fig.8 (d)), 30.84dB (Fig.9 (b)), 30.84dB (Fig.9 (d)), 30.84dB (Fig.10 (b)), 30.84 dB (Fig.10 (d)), 30.84dB (Fig.11 (b)), 30.84dB (Fig.11 (d)). Fig. 12 shows the graphical representation for variation of PSNR after modulation of different channels and different levels of subbands. The graphical representation also shows the visual quality of the decoded image with and without the usage of the extracted key. The numerical values of PSNR are computed by averaging over all the test images. Table 4 - 6 list the B.R., C.R., PSNR and MSSIM values for various images like Pepper, Lena, Water and House. From the numerical values shown in Table 4-6 and the graphical representation shown in Fig. 12, it is quite clear that data modulation on ROI is reverted completely and the full quality of image is restored without increasing any bit rate.

Table 4: Results for different images if only Y channel is modulated by the key and are decoded without and with the true key.

Name of image		Case- 1				Case- 2				Case- 3			
		Lena	Pepper	House	Water	Lena	Pepper	House	Water	Lena	Pepper	House	Water
Without key	PSNR	29.07	28.24	26.77	28.01	25.87	25.54	23.58	26.23	22.70	23.11	21.78	24.90
	MSSIM	0.88	0.87	0.86	0.81	0.81	0.82	0.79	0.74	0.75	0.76	0.74	0.70
	B.R.	1.36	1.48	1.50	1.52	1.36	1.48	1.50	1.52	1.36	1.48	1.50	1.52
	C.R.	9.36:1	7.51:1	8.40:1	9.05:1	9.36:1	7.51:1	8.40:1	9.05:1	9.36:1	7.51:1	8.40:1	9.05:1
With key	PSNR	33.34	30.84	30.56	30.53	33.34	30.84	30.56	30.53	33.34	30.84	30.56	30.53
	MSSIM	0.92	0.92	0.92	0.88	0.92	0.92	0.92	0.88	0.92	0.92	0.92	0.88

Table 5: Results for different images if only  $C_b$  or  $C_r$  channel is modulated by the key and are decoded without and with the true key.

Name of image		Chrominance ( $C_b$ ) component				Chrominance ( $C_r$ ) component				
		Lena	Pepper	House	Water	Lena	Pepper	House	Water	
Case-2	Without key	PSNR	32.91	30.56	30.36	30.38	32.85	29.63	30.05	30.07

Case-2	Without key	MSSIM	0.92	0.91	0.92	0.88	0.92	0.90	0.92	0.87
		B.R.	1.36	1.48	1.50	1.52	1.36	1.48	1.50	1.52
		C.R.	9.36:1	7.51:1	8.40:1	9.05:1	9.36:1	7.51:1	8.40:1	9.05:1
	With key	PSNR	33.34	30.84	30.56	30.53	33.34	30.84	30.56	30.53
		MSSIM	0.92	0.92	0.92	0.88	0.92	0.92	0.92	0.88
Case-3	Without key	PSNR	31.92	29.78	29.36	30.10	32.09	28.07	29.51	29.65
		MSSIM	0.92	0.90	0.91	0.87	0.91	0.88	0.91	0.86
		B.R.	1.36	1.48	1.50	1.52	1.36	1.48	1.50	1.52
		C.R.	9.36:1	7.51:1	8.40:1	9.05:1	9.36:1	7.51:1	8.40:1	9.05:1
	With key	PSNR	33.34	30.84	30.56	30.53	33.34	30.84	30.56	30.53
		MSSIM	0.92	0.92	0.92	0.88	0.92	0.92	0.92	0.88

Table 6: Results for different images if both  $C_b$  and  $C_r$  or all i.e.  $Y, C_b$  and  $C_r$  channels are modulated by the key and are decoded without and with the true key.

Name of image		$C_b$ and $C_r$				$Y, C_b$ and $C_r$				
		Lena	Pepper	House	Water	Lena	Pepper	House	Water	
Case-2	Without key	PSNR	32.48	29.42	29.88	29.97	25.47	25.33	23.46	25.99
		MSSIM	0.92	0.89	0.91	0.87	0.80	0.82	0.78	0.73
		B.R.	1.36	1.48	1.50	1.52	1.36	1.48	1.50	1.52
		C.R.	9.36:1	7.51:1	8.40:1	9.05:1	9.36:1	7.51:1	8.40:1	9.05:1
	With key	PSNR	33.34	30.84	30.56	30.53	33.34	30.84	30.56	30.53
		MSSIM	0.92	0.92	0.92	0.88	0.92	0.92	0.92	0.88
Case-3	Without key	PSNR	31.03	27.47	28.62	29.36	22.37	22.65	21.44	24.62
		MSSIM	0.90	0.86	0.90	0.86	0.74	0.75	0.72	0.69
		B.R.	1.36	1.48	1.50	1.52	1.36	1.48	1.50	1.52
		C.R.	9.36:1	7.51:1	8.40:1	9.05:1	9.36:1	7.51:1	8.40:1	9.05:1
	With key	PSNR	33.34	30.84	30.56	30.53	33.34	30.84	30.56	30.53
		MSSIM	0.92	0.92	0.92	0.88	0.92	0.92	0.92	0.88

Fig. 13 shows the graphical representation for the comparison of image quality in term of PSNR values for watermarks (secret key) of different lengths. Simulation results show that lifting offers advantages of low loss in image information for QIM data embedding. The overall improvement in visual quality through higher PSNR values compared to normal DWT is achieved due to lossless integer coefficient conversion. Moreover, the correlations among the sample coefficients is the other reason for visual quality improvement due to the use of lifting and can be well explained by Equation 2 and Equation 3. The use of lifting offers further benefits on access control over normal DWT coefficients through lower values of decoding error for the embedded watermark. To test the bit error rate (BER)  $P_e$  of the extracted key/watermark, some typical common signal processing operations are performed on large number of images. The numerical values of BER are averaged and are shown in Table 7. The BER values in turn play the key role in access control where low BER offers better quality of the images through the demodulation of ROI coefficients. It is seen that the values of  $P_e$ , against most of the common signal processing operations, are low for lifting based data hiding compared to the same for normal DWT. The improved results are achieved due to the low values of variance for lifting based DWT coefficients compared to normal DWT coefficients and is shown in Table 8. In other words, better visual quality of image is achieved for the former through the proposed access control scheme.

Table 7: Bit error rate ( $P_e$ ) for normal and lifting based DWT (A: JPEG 85; B: Median (3x3); C: Mean (3x3);D: High pass (3x3); E: Down & Up (.9) ;F: Histogram; G: Dynamic Range; H: Salt & Pepper (.009) ;I: Speckle (.009);J: Gaussian (.009))

	A	B	C	D	E	F	G	H	I	J
DWT	0	0.64	0.74	0	0.78	0.52	0	0	0.14	0.40
Lifting	0	0.31	0.39	0	0.19	0.33	0	0	0.12	0.38

Table 8: The variance values for different subbands of several image due to lifting based DWT and normal DWT decomposition

Image	Lifting (Haar)		DWT ( Haar)	
	HL2	LH2	HL2	LH2
Pepers	33.1807	23.2676	127.2946	86.7732
Lena	3.4287	9.0786	11.2725	32.6170
Kids	4.3397	3.0419	15.2221	9.4108
Water	6.6178	5.5664	23.4879	17.9872

Results shown in Table 4-6 highlight the fact that modulation in lifting based DWT coefficients up to three levels is enough for access control as this amount of distortion is sufficient for quality access control of images. This fact is also supported by the simulation results obtained after the required experimentation done over four other test images and the objective measure of visual quality are reported in Table 9-10. Figs.14 (a)-(d) further support the above fact subjectively through various tests done over the test image 'kid'.

Table 9: Results for different images without watermarking and quality access control mechanism.

Image	Only Compression				Compression With Watermarking			
	B.R.	C.R.	PSNR	MSSIM	B.R.	C.R.	PSNR	MSSIM
Boat	1.59	7.62:1	30.39	0.92	1.57	8.40:1	30.26	0.91
Kid	1.19	9.96:1	34.96	0.94	1.17	10.96:1	34.82	0.94
Opera	1.23	11.08:1	34.24	0.93	1.21	12.25:1	34.20	0.94
Paper machine	1.46	11.77:1	31.95	0.93	1.44	12.92:1	31.93	0.93

Table 10: Results for different images if all bands (case-3) are modulated by the key and decoded without and with the true key.

	Images	Boat	Kid	Opera	Paper m/c	Boat	Kid	Opera	Paper m/c
		$Y$				$C_r$			
Without key	PSNR	21.89	23.71	25.37	19.55	29.06	33.78	33.90	31.60
	MSSIM	0.74	0.77	0.72	0.73	0.90	0.93	0.92	0.93
	B.R.	1.57	1.17	1.21	1.44	1.57	1.17	1.21	1.44
	C.R.	8.40:1	10.96:1	12.25:1	12.92:1	8.40:1	10.96:1	12.25:1	12.92:1
With key	PSNR	30.26	34.82	34.20	31.93	30.26	34.82	34.20	31.93
	MSSIM	0.91	0.94	0.94	0.93	0.91	0.94	0.94	0.93
Without key	$C_b$					$Y, C_b \text{ \& } C_r$			
	PSNR	29.59	34.00	33.85	31.76	21.94	23.59	25.31	19.54
	MSSIM	0.90	0.93	0.92	0.93	0.75	0.77	0.72	0.72
	B.R.	1.57	1.17	1.21	1.44	1.57	1.17	1.21	1.44
	C.R.	8.40:1	10.96:1	12.25:1	12.92:1	8.40:1	10.96:1	12.25:1	12.92:1
With key	PSNR	30.26	34.82	34.20	31.93	30.26	34.82	34.20	31.93
	MSSIM	0.91	0.94	0.94	0.93	0.91	0.94	0.94	0.93

We also compare the performance of our access control method with the results obtained in [8, 29] in terms of coding rate, key correction ratio(KCR), PSNR and MSSIM in the presence of bit error rate(BER). The word BER here implies the error in the received compressed signal when transmitted through the noisy channel or manipulated by some user. The BER is simulated in this experimentation by randomly manipulating the compressed data. This affects PSNR and MSSIM values of the received image with respect to the compressed version. KCR can be defined as the percentage of match between the true key and the extracted key. It is observed from Table 11 that our scheme can extract the key correctly (high value of KCR) in the presence of various bit error and also decode the image effectively. Simulation results show that our method can decode the key correctly even at BER of  $10^{-4}$  for the compressed modulated data and offers better PSNR and MSSIM values at low coding rate. It is also to be pointed out that PSNR for Chang [8]

method is little better compared to our method but the coding rate of the former is much higher than the latter. This, in other words, shows that high PSNR in [29] is possible when there is no compression while our method allows significant compression (low bit rate) even at reasonable good visual quality. The results of the proposed scheme is also compared with the results obtain in [30] and JPEG 2000 compression with ROI coding. The results shown in Table 12 highlight that our access control method not only offers better overall PSNR values compared to [30] and JPEG 2000, but also protect ROI through access control in a much better way compared to [30].

Table 11: Comparison of results for Coding rate, KCR, PSNR, MSSIM.

	Coding Rate (bits/pixel)	KCR (Key Correction Ratio %)			BER=10 <sup>-4</sup>	
		BER=10 <sup>-4</sup>	BER=10 <sup>-5</sup>	BER=10 <sup>-6</sup>	PSNR	MSSIM
Chang[8]	8	76	99	100	35.74	0.962
Zaidee[29]	1.24	99	99	100	28.84	0.910
Proposed	1.36	100	100	100	34.55	0.958

Table 12: Comparison of coding results after decoding.

	Bit rate	PSNR(dB)		PSNR(dB)
		ROI	non-ROI	Overall
Fukuma et al [30]	0.35	33.10	26.10	26.90
JPEG 2000	0.35	45.40	19.90	19.00
Proposed	0.82	46.42	35.05	28.20

Fig. 15 is an illustration of decoding reliability for the proposed method using different fake key (brute force attacker). It is seen that without the correct key, the decoded images are of poor qualities than the images when decoded by the true key. It demonstrates that our scheme is sensitive to key and hence it is secured. It is difficult for the attackers/unauthorized users to enjoy the original quality of the image without knowing the exact key. It means only authentic user can avail full quality.

## 4 Conclusions and Scope of Future Works

An efficient algorithm for quality access control of compressed color image is proposed in this work by modulating the ROI coefficients and subsequent embedding of modulation information (key) in the chrominance blue-channel into the non-ROI region. The usage of lifting based DWT offers low computation cost, low loss in image quality and better decoding reliability for the embedded data over normal DWT. The decoding reliability offers better access control and the fact is supported by mathematical analysis as well as through extensive simulation results. Simulation results show that the authorized users having the full knowledge of the secret key restore the full quality of ROI. Simulation results also show that protection of ROI for the proposed method is much better compared to other existing access control scheme. Future work may be done to extend the proposed access control method for compressed video and audio signal, as well as development of hardware implementation of the proposed access control scheme through application specific integrated circuit (ASIC) or field programmable gate array (FPGA).

## References

- [1] F.A.P.Petitcolas, H.J.Kim, *Digital Watermarking*, Springer-Verleg, 2003.
- [2] S. P. Maity, M. K. Kundu, S. Maity, "Dual purpose FWT domain spread spectrum image watermarking in real-time", *International Journal of Computer & Electrical Engineering in the special issue on Real-Time Security and Copyright Protection of Multimedia*, Elsevier Science,35(2): 415-433, 2009.
- [3]P. Campisi, M. Carli, G.Giunta, A. Neri, "Blind quality assessment system for multimedia communications using tracing watermarking", *IEEE Transaction on Signal Processing*, 51(4): 996-1002,2003.

- [4] C. Jin, J. Peng, "Robustness of a blind image watermark detector designed by orthogonal projection", *Electronic Letters on Computer Vision and Image Analysis*, 4(1):11-20, 2004.
- [5] C.K. Yang, C.S. Huang, "A novel watermarking technique for tampering detection in digital images", *Electronic Letters on Computer Vision and Image Analysis*, 3(1): 1-12, 2004.
- [6] R. Grosbois, P. Gerbelot, T. Ebrahimi, "Authentication and access control in the JPEG 2000 compressed domain", *SPIE Proc. of 46<sup>th</sup> Annual Meeting Applications of Digital Image Processing XXIV*, San Diego, 95-104, 2001.
- [7] S. Imaizumi, O. Watanabe, M. Fujiyoshi, H. Kiya, "Generalized hierarchical encryption of JPEG 2000 code streams for access control", *IEEE Proc. of Conf. On Image Processing*, Genoa, Italy, 2:1094-7, 2005.
- [8] F.C. Chang, H.C. Huang, H. M. Hang, "Layered access control schemes on watermarked scalable media", *Journal of VLSI Signal Processing* (Springer Netherlands), 49(3): 443 – 455, 2007.
- [9] M. Pickering, L.E. Coria, P. Nasiopoulos, "A novel blind video watermarking scheme for access control using complex wavelets", *IEEE Proc. of Conf. on Consumer Electronics*, Las Vegas, NV, 1-2, 2007.
- [10] A. Phadikar, M.K. Kundu, S.P. Maity, "Quality access control of a compressed gray scale image", *Proc. of Conf. On Computer Vision, Pattern Recognition, Image Processing and Graphics (NCVPRIPG 08)*, India, 13-19, 2008.
- [11] X. Wu, J. Hu, Z. Gu, J. Huang, "A secure semi-fragile watermarking for image authentication based on integer wavelet transform with parameters", *Proc. of the 2005 Australian Workshop on Grid Computing And E-Research*, New South Wales, Australia 4:75-80,2005.
- [12] P.Meerwald, A.Uhl, "A survey of wavelet-domain watermarking algorithms", *SPIE Proc. of Conf. On Electronic Imaging, Security and Watermarking of Multimedia Contents*, San Jose, CA, USA, 505-516 2001.
- [13] Y.H. Seo, D.W. Kim, "A new VLSI architecture of lifting-based DWT", *Lecture Notes in Computer Science*, 3985:146-151, 2006.
- [14] A. Phadikar, S. P. Maity, M. K. Kundu, "Quantization based data hiding scheme for efficient quality access control of images using DWT via lifting", *IEEE Proc. of 6<sup>th</sup> Indian Conf. on Computer Vision, Graphics and Image Processing (ICVGIP'08)*, Bhubaneswar, India, 266-272,2008.
- [15] B. Chen, G. W. Wornell, "Quantization index modulation: a class of provably good methods for digital watermarking and information embedding", *IEEE Transaction on Information Theory*, 47(4): 1423: 1443, 2001.
- [16] D. S. Taubman , M. W. Marcellin, *JPEG 2000: Fundamentals, Standards and Practice*, Kluwer Academic Publishers, Boston, 2002.
- [17] W. Sweldens, "The lifting scheme: a custom- design construction of biorthogonal wavelets", *Applied and Computational Harmonic Analysis*, 3(2): 186-200, 1996.
- [18] W. Sweldens, "The lifting scheme: construction of second generation wavelets", *SIAM Journal on Mathematical Analysis*, 29(2): 511-546, 1997.
- [19] J. Kovacevic, W. Sweldens, "Wavelet families of increasing order in arbitrary dimensions", *IEEE Transaction on. Image Processing*, 9 (3):480-496, 2000.
- [20] M Boliek, C. Christopoulos, E. Majani, "JPEG2000 part I final draft international standard", (ISO/IEC FDIS15444-1), ISO/IEC JTC1/SC29/ WG1 N1855, 2000.
- [21] M. D. Adams, F. Kossentini, "Reversible integer-to-integer wavelet transforms for image compression: performance evaluation and analysis", *IEEE Transaction on Image Processing*, 9(6):1010-1024, 2000.
- [22] S.Voloshynovskiy, T.Pun, "Capacity security analysis of data hiding technologies", *IEEE Proc. of Conf. on Multimedia and Expo*, Lausanne, Switzerland, pp. 477-480, 2002.
- [23] C. Christopoulos, A. Skodras,T. Ebrahimi, "The JPEG 2000 still image coding system: an overview", *IEEE Transactions on Consumer Electronics*, 46(4): 1103-1127, 2000.
- [24] M. Barni, F. Bartolini, A. Piva, "Improved wavelet-based watermarking through pixel-wise masking" *IEEE Transactions on Image Processing*, 10(5):783-791,2001.
- [25] <http://www.cl.cam.ac.uk/fapp2/watermarking>.
- [26] [http://www.petitcolas.net/fabien/watermarking/image\\_database/index.html](http://www.petitcolas.net/fabien/watermarking/image_database/index.html).
- [27] R.C. Gonzalez, R.E. Woods, S.L. Eddins, *Digital Image processing using Matlab*, 2<sup>nd</sup> ed. Prentice Hall, Upper Saddle River, NJ,2005.

- [28] Z. A. Wang, C. Bovik, H. R. Sheikh, E. P. Simoncelli, "Image quality assessment: from error measurement to structural similarity", *IEEE Transactions on Image Processing*, 13(1): 1-14, 2004.
- [29] A.A. Zaidee, S. Fazdliana, B.J. Adznan, "Content access control for JPEG images using CRND zigzag scanning and QBP", *IEEE Proc. of 6<sup>th</sup> Conf. On Computer and Information Technology*, Bangalore, India 146 – 146, 2006.
- [30] S. Fukuma, M. Ito, C. Imajo, S. Nishimura, M. Nawate, "A relative quality controlled region-of-interest image coding based on wavelet transform", *IEEE Proc. of 45<sup>th</sup> Midwest Symposium on Circuits and Systems*, Tulsa, OK, USA 1:459-62,2002.

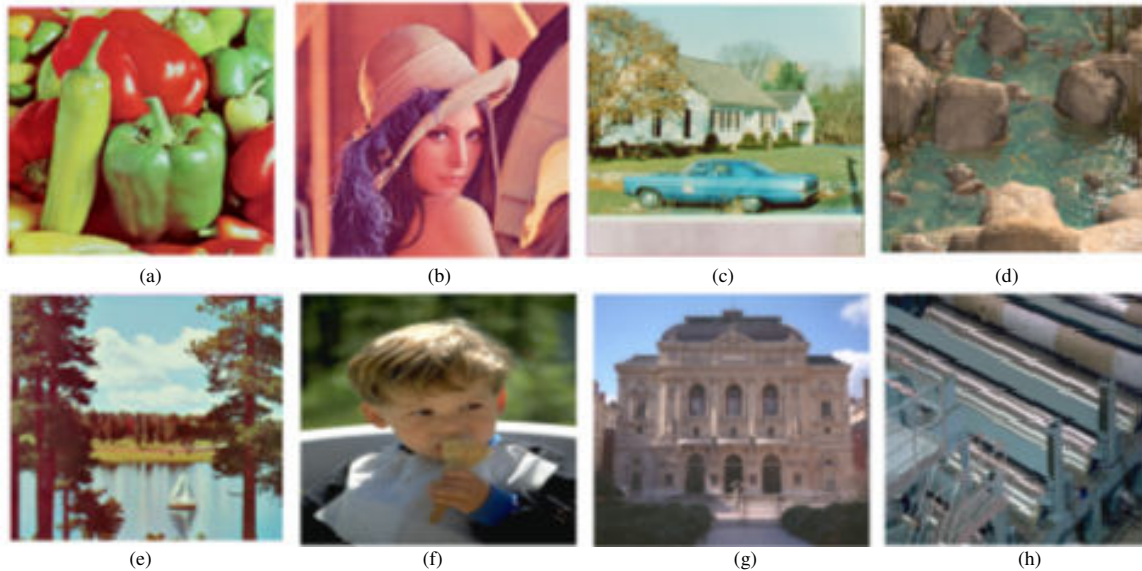


Figure 6: Test images. (a) Pepper; (b) Lena; (c) House; (d) Water ; (e) Boat ; (f) Kid; (g) Opera; (h) Paper machine.

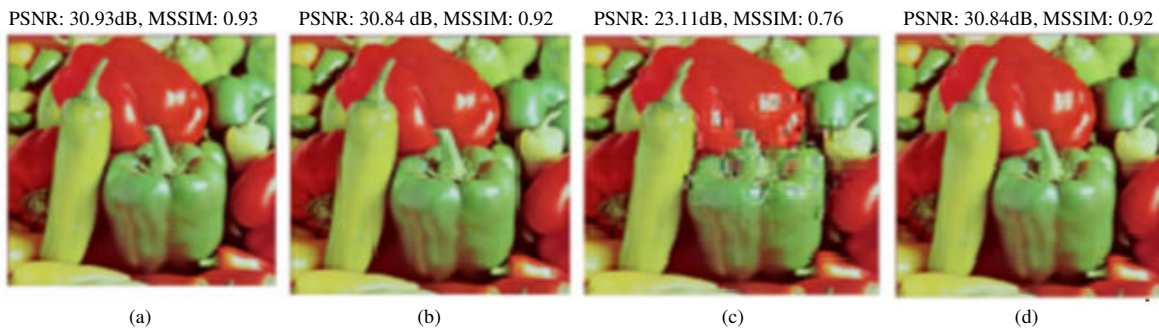


Figure 7: (a) Decompressed test image, (b) Decompressed watermarked image; Results if only luminance (Y) component is modulated by the key (c) & (d): accesses control for case-3, (c) decoded image without key, (d) decoded image with the true key.

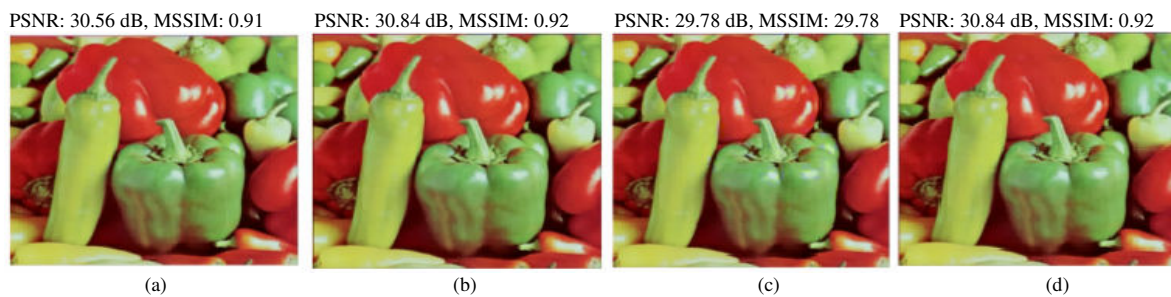


Figure 8: Results if only chrominance ( $C_b$ ) component is modulated by the key (a) & (b): quality accesses control for case-2, (a) decoded image without key, (b) decoded image with the true key, (c) & (d): quality accesses control for case-3, (c) decoded image without key, (d) decoded image with the true key.

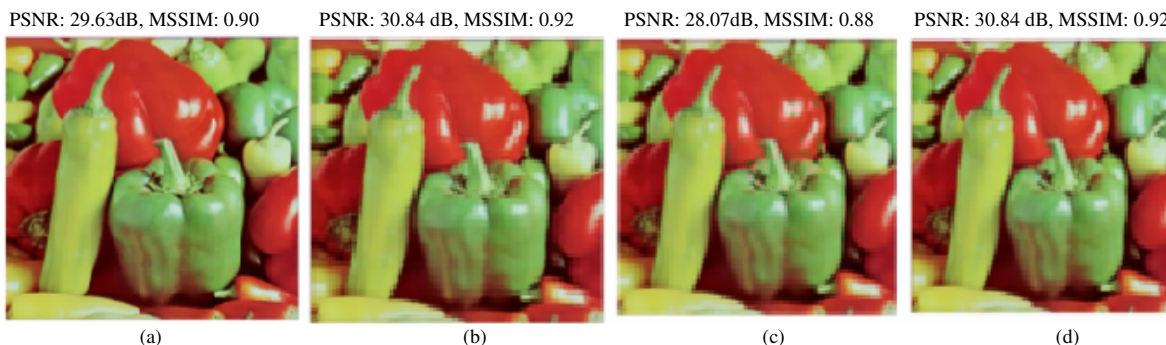


Figure 9: Results if only chrominance ( $C_r$ ) component is modulated by the key (a) & (b): quality accesses control for case-2, (a) decoded image without key, (b) decoded image with the true key, (c) & (d): quality accesses control for case-3, (c) decoded image without key, (d) decoded image with the true key.

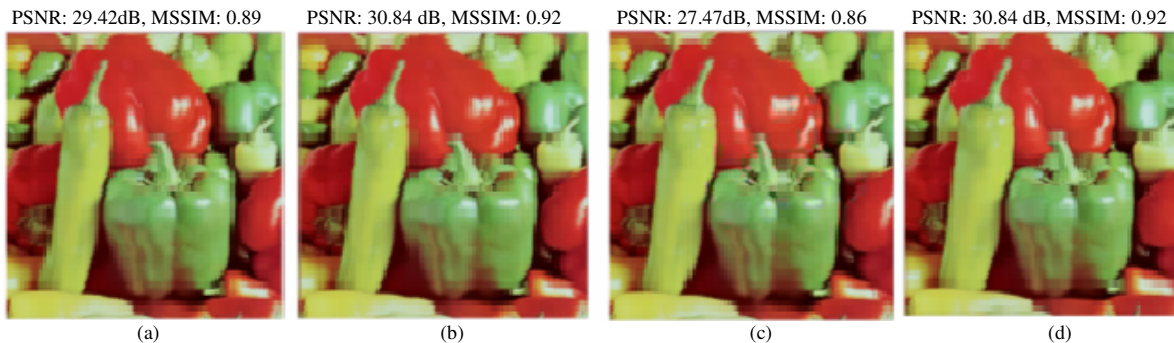


Figure 10: Results if both chrominance ( $C_b$ ) and chrominance ( $C_r$ ) components are modulated by the key (a) & (b): quality accesses control for case-2, (a) decoded image without key, (b) decoded image with the true key, (c) & (d): quality accesses control for case-3, (c) decoded image without key, (d) decoded image with the true key.

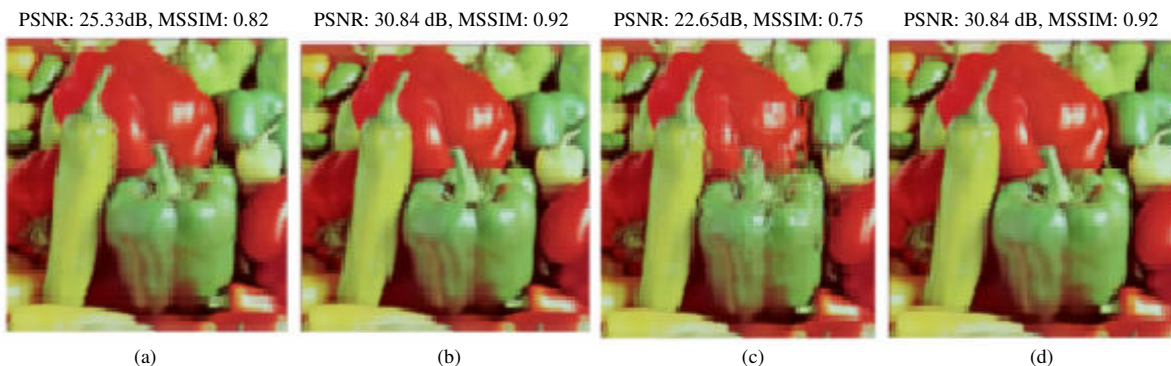


Figure 11: Results if luminance ( $Y$ ), chrominance ( $C_b$ ) and chrominance ( $C_r$ ) components are modulated by the key (a) & (b): quality accesses control for case-2, (a) decoded image without key, (b) decoded image with the true key, (c) & (d): quality accesses control for case-3, (c) decoded image without key, (d) decoded image with the true key.

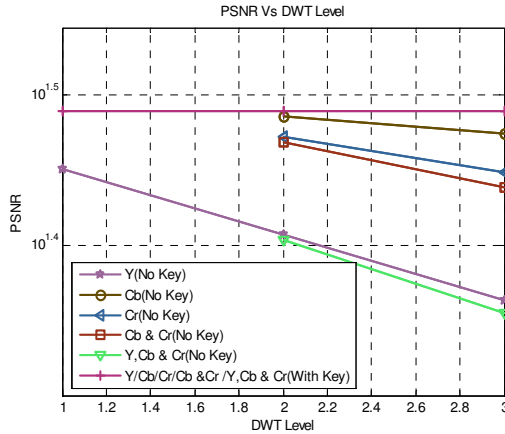


Figure 12: Results of PSNR for different cases of a test image (Pepper).

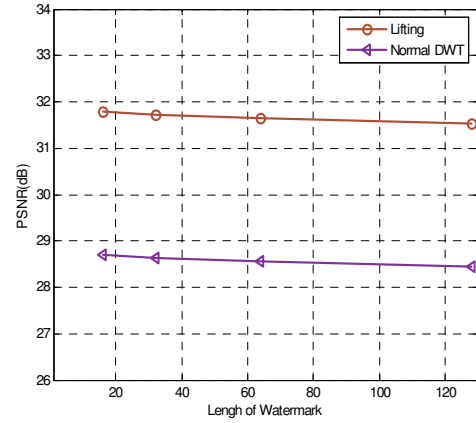


Figure 13: Results of PSNR for different cases of a test image (Pepper).

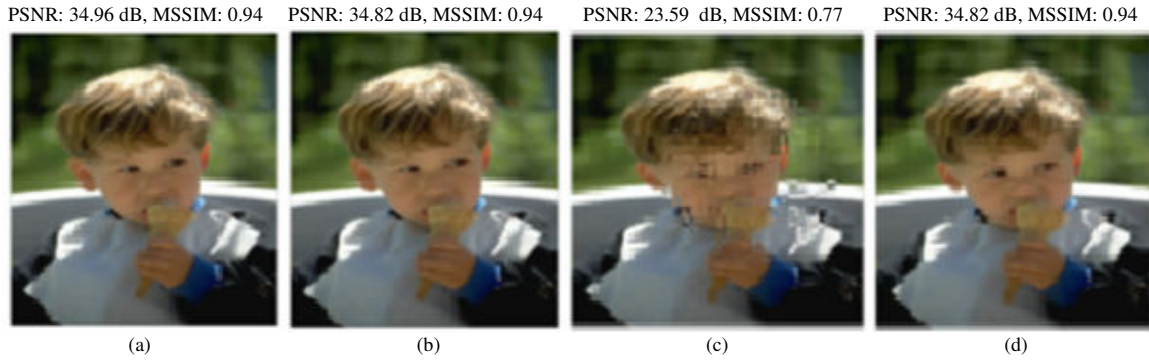


Figure 14: (a) Decompressed test image, (b) Decompressed watermarked image, (c) & (d): Results of modulation in luminance ( $Y$ ), chrominance ( $C_b$ ) and chrominance ( $C_r$ ) components for case-3, (c) decoded image without key, (d) decoded image with the true key.

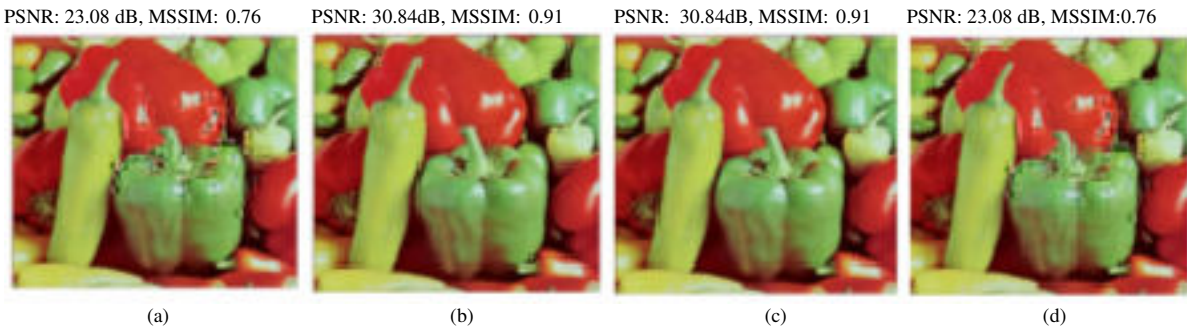


Figure 15: Results for test image 'Pepper' if decoded by false (a random) key (case-3 i.e. when all subbands are modulated), (a): decoded image with false key if only  $Y$  channel is modulated, (b): decoded image with false key if only  $C_b$  channel is modulated, (c): decoded image with false key if only  $C_r$  channel is modulated, (d): decoded image with false key if all channels i.e.  $Y, C_b, C_r$  are modulated.